2886 *Inorg. Chem.* **1993**, *32*, 2886–2893

Synthesis and Structures of Polar Coordination Polymers: [(SALEN)MnO$_2$CCH$_2$D-B:]$_n$ (D = NH, S; -B: = 4-Pyridyl, 4-Cyanophenyl)

William Chiang, Douglas M. Ho, Donna Van Engen, and Mark E. Thompson*

Department of Chemistry, Princeton University, Princeton, New Jersey 08544

Received August 14, 1992

Reaction between [*N*,*N*′-ethylenebis(salicylaldiminato)]manganese(III) bromide (Mn(SALEN)Br) and *N*-4-pyridylglycine gives Mn(SALEN)(*N*-4-pyridylglycinate) (**1**), which crystallizes as an infinite-chain coordination polymer. The polymer chains consist of metal centers bridged by 4-pyridylglycinate ligands. The Mn atoms are octahedrally coordinated with the SALEN ligand filling four equatorial sites, a carboxylate oxygen occupying one axial site, and a pyridyl nitrogen of an adjacent molecule occupying a trans axial site. This bonding pattern is repeated to give a polymer with head-to-tail alignment along the backbone. The reaction between Mn(SALEN)Br and (4-pyridylthio)acetic acid gives the compound Mn(SALEN)((4-pyridylthio)acetate) (**2**), with a polymeric structure in the solid state very similar to that of **1**. **1**, $C_{24}H_{27}MnN_4O_6$, crystallizes in the monoclinic space group $P2_1/c$ with a = 10.782(2) Å, b = 18.100(6) Å, c = 12.886(4) Å, β = 105.22(2)°, and Z = 4. **2**, $C_{23}H_{22}MnN_3O_5S$, crystallizes in the monoclinic space group $P2_1/c$ with a = 10.670(1) Å, b = 17.754(3) Å, c = 12.714(2) Å, β = 108.78(1)°, and Z = 4. In contrast, the reaction of Mn(SALEN)Br with *N*-(4-cyanophenyl)glycine gives **3**, whose crystal structure consists of a mixture of the monomeric (H_2O)Mn(SALEN)(*N*-(4-cyanophenyl)glycinate) and a Mn(SALEN)(*N*-(4-cyanophenyl)glycinate) polymer. This polymer consists of adjacent Mn(SALEN) moieties bridged by a single carboxylate unit in a syn-anti conformation; thus no head-to-tail alignment is observed along the backbone. **3**, $C_{25}H_{21}MnN_4O_4{\cdot}C_{25}H_{23}MnN_4O_5$, crystallizes in the monoclinic space group $P2_1/n$, with a = 14.295(4) Å, b = 11.614(4) Å, c = 27.220(7) Å, β = 90.20(2)°, and Z = 4.

Introduction

The field of nonlinear optics is one of the fastest growing areas of research today. One reason for this growth is the continuing need for materials with larger nonlinear optical coefficients, so that less intense light sources can be used and optical components can be made as small as possible.[1] The first solids to demonstrate second-order nonlinear optical (NLO) properties were inorganic crystals (e.g. quartz, $LiNbO_3$, and KH_2PO_4).[2] Several years later, it was found that organic compounds (e.g. 2-methyl-4-nitroaniline) could have significantly higher NLO coefficients[3] and damage thresholds[4] than inorganic compounds. This increase in NLO coefficients is due partly to the high polarizability of the π-electron network commonly found in organic compounds. In addition, organic compounds are easily substituted with acceptor and donor groups to give them dipolar character in either the ground or excited state, leading to large second-order nonlinearities. Recently, organometallic and coordination complexes with good NLO coefficients have been reported as well.[5] Second harmonic generation (SHG, frequency doubling) and the electro-optic effect are two common second-order NLO processes.[6]

For a molecular solid to demonstrate second-order NLO properties, it must be composed of molecules with high molecular NLO susceptibilities packed in a head-to-tail manner so that their dipolar nature is extended to the bulk solid. If such a polar structure is not formed, the material will not demonstrate any second-order NLO properties.[2f,7] The requirement that a material crystallize in a polar space group has an impact on the NLO properties of most molecular materials, since a majority of all molecules crystallize in a centrosymmetric space group.[8] A number of approaches to the preparation of polar materials have been used. Hydrogen bonding,[9] Langmuir–Blodgett techniques,[10] poled polymers,[11] and inclusion phenomena[12] have all been used with limited success. Electric field poling polymer composites

---

(1) (a) Prasad, P. N.; Williams, D. J. *Nonlinear Optical Effects in Molecules and Polymers*; John Wiley and Sons, Inc.: New York, 1991. (b) Ulrich, D. R. *Mol. Cryst. Liq. Cryst.* **1990**, *189*, 3. (c) Simon, S.; Bassoul, P.; Norvez, S. *New J. Chem.* **1989**, *13*, 13. (d) Glass, A. M. *Science* (*Washington, D.C.*) **1984**, *226*, 557.

(2) (a) Franken, P. A.; Hill, A. E.; Peters, C. W. *Phys. Rev. Lett.* **1961**, *7*, 118. (b) Miller, R. C.; Kleinman, D. A.; Savage, A. *Phys. Rev. Lett.* **1963**, *11*, 146. (c) Miller, R. C. *Phys. Rev. Lett.* **1964**, *5*, 17. (d) Boyd, G. D.; Miller, R. C.; Nassau, K.; Bond, W. L.; Savage, A. *Appl. Phys. Lett.* **1964**, *5*, 234. (e) Miller, R. C.; Boyd, G. D.; Savage, A. *Appl. Phys. Lett.* **1965**, *6*, 77. (f) For a review see: Chen, C.; Liu, G. *Annu. Rev. Mater. Sci.* **1986**, *16*, 203.

(3) (a) Lipscomb, G. F.; Garrito, A. F.; Narang, R. S. *J. Chem. Phys.* **1981**, *75*, 1509. (b) Levine, B. F.; Betha, C. G.; Thurmond, C. D.; Lynch, R. T.; Bernstein, J. L. *J. Appl. Phys.* **1979**, *50*, 2523. (c) Chemla, D. S.; Zyss, J. *Organic Materials for Nonlinear Optics*; Academic Press, Inc.: London, 1987; Vol. 1.

(4) (a) Baumert, J. C.; Tweig, R. J.; Bjorklund, G. C.; Logan, J. A.; Dirk, C. W. *Appl. Phys. Lett.* **1987**, *51*, 1484. (b) Huggard, P. G.; Blau, W.; Schweitzer, D. *Appl. Phys. Lett.* **1987**, *51*, 2183. (c) Zyss, J. *J. Mol. Electron* **1985**, *1*, 24.

(5) (a) Tam, W.; Calabrese, J. C. *Chem. Phys. Lett.* **1988**, *44*, 79. (b) Green, M. L. H.; Marder, S. R.; Thompson, M. E.; Bandy, J. A.; Bloor, D.; Kolinsky, P. V.; Jones, R. J. *Nature* **1987**, *330*, 360. (c) For a review on organometallics for NLO see: Nalwa, H. S. *Appl. Organomet. Chem.* **1991**, *5*, 349.

(6) Prasad, P. N.; Williams, D. J. *Nonlinear Optical Effects in Molecules and Polymers*; John Wiley and Sons, Inc.: New York, 1991; Chapter 5 and references therein.

(7) Williams, D. J. *Angew. Chem., Int. Ed. Engl.* **1984**, *23*, 690.

(8) Desiraju, G. R. *Crystal Engineering: The Design of Organic Solids*; Elsevier Science Publishers: Amsterdam, 1989.

(9) (a) Etter, M. C.; Frankenbach, G. M. *Chem. Mater.* **1989**, *1*, 10. (b) Panunto, T. W.; Urbanczk-Lipkowska, Z.; Johnson, R.; Etter, M. C. *J. Am. Chem. Soc.* **1987**, *109*, 7786.

(10) (a) Popovitz-Biro, R.; Hill, K.; Landau, E. M.; Lahav, M.; Leiserowitz, L.; Sagiv, J. *J. Am. Chem. Soc.* **1988**, *110*, 2672. (b) Cross, G. H.; Peterson, I. R.; Girling, I. R.; Cade, N. A.; Goodwin, M. J.; Carr, N.; Sethi, R. S.; Marsen, R.; Gray, G. W.; Lacey, D.; McRoberts, M.; Scrowston, R. M.; Toyne, K. J. *Thin Solid Films* **1988**, *156*, 39. (c) Richardson, T.; Roberts, G. G.; Polywka; Davies, S. G. *Thin Solid Films* **1988**, *160*, 231. (d) Ledoux, I.; Fremaux, P.; Piel, J. P.; Post, G.; Zyss, J.; McLean, T.;Hann, R. A.; Gordon, P. F.; Allen S. *Thin Solid Films* **1988**, *160*, 217. (e) Swalwn, J. D. *Thin Solid Films* **1988**, *160*, 197.

(11) (a) Ye, C.; Minami, N.; Marks, T. J.; Yang, J.; Wong, G. K. *Macromolecules* **1988**, *21*, 2901. (b) Hampsch, H. L.; Yang, J.; Wong, G. K.; Torkelson, J. M. *Macromolecules* **1988**, *21*, 526. (c) Meredith, G. R.; VanDusen, J. G.; Williams, D. J. *Macromolecules* **1982**, *15*, 1385.

(12) (a) Tam, W.; Eaton, D. F.; Calabrese, J. C.; Williams, I. D.; Wang, Y.; Anderson, A. G. *Chem. Mater.* **1989**, *1*, 128. (b) Wang, Y.; Eaton, D. F. *Chem. Phys. Lett.* **1985**, *120*, 441. (c) Tomaru, S.; Zembutsu, S.; Kawachi, M.; Kobayashi, M. *J. Chem. Soc., Chem. Commun.* **1984**, 1207.

0020-1669/93/1332-2886$04.00/0

and Langmuir–Blodgett techniques have been the most successful at aligning molecules but have led to materials with limited thermal stability, relative to crystalline materials. Our approach to the development of new second-order NLO materials is to synthesize inorganic coordination polymers where molecules are aligned in a head-to-tail arrangement along the polymer backbone.

Square pyramidal transition metal complexes usually adopt an octahedral configuration in solution by coordinating a solvent molecule. In the solid state, the sixth coordination site can be filled by a Lewis basic ligand of an adjacent molecule, giving a coordination polymer (e.g. eq 1).[13] This type of coordination in

$$Cl_4M{=}O(soln) \rightarrow Cl_4M{=}O{\rightarrow}Cl_4M{=}O{\rightarrow}Cl_4M{=}O(s) \qquad (1)$$

$$M = Mo, W$$

the solid state is very common for metal nitrides and oxides.[14] The head-to-tail nature of coordination may make it an ideal method for preparing polar chains. The organization in these materials is similar to that found in hydrogen-bonded systems. Hydrogen-bonding acceptors and donors are incorporated into a molecule, leading to head-to-tail alignment of the molecules (e.g. 3,4-diamino-2,4,6-trinitrophenol).[15] An advantage that coordination polymers may have over hydrogen-bonded systems is that the coordinate bond is typically much stronger than a hydrogen bond. The formation of the coordinate bond will have a stronger influence in directing the crystallization into the desired polar chains. Furthermore, it may be possible to alter the electronic properties of the material without significantly affecting the solid-state structure by changing the metal center.

Recently Hopkins et al. have reported the second-order NLO properties for a series of Mo and W nitride coordination polymers [$(RO)_3M{\equiv}N$; M = Mo, R = CMe_3, CMe_2CF_3; M = W, R = CMe_3].[16] These complexes crystallize in polar space groups with infinite metal–nitride chains [$\rightarrow M{\equiv}N \rightarrow M{\equiv}N \rightarrow M{\equiv}N$; M = $(RO)_3Mo$] parallel to the *c* axis.[17] Easily detectable but weak SHG signals were observed for all of the complexes. One possible explanation for the weakness of the SHG signal is that the NLO chromophores have low nonlinear coefficients, since NLO properties depend strongly on the size of the chromophore.[18] The $M{\equiv}N$ unit may be polarizable and have favorable ground- and excited-state dipole moments, but the length of the π system is very short (1.66–1.74 Å). The goal of the chemistry described herein is to prepare and study coordination complexes with an extended π system joining an organic donor and a metal atom acceptor. In these complexes, coordination polymerization will lead to polar order along the polymer axis.

Results and Discussion

In designing monomers for crystallization into coordination polymers for second-order NLO, one needs to consider a number of important features. The complexes used in our study are pictured in Figure 1a,b and will be used to illustrate each of the considerations. In the crystalline polymer (Figure 1c), the donor is connected to one metal ion by a pyridyl group, whose π system will facilitate a strong donor–acceptor interaction. In the opposite direction, the donor is insulated from the metal ion by an aliphatic group. Without this insulation, the donor would interact with both metal ions simultaneously, diminishing the net effect. Our monomers have a square pyramidal structure with the bridging ligand at its apex. This conformation will prevent dimer formation and encourage a linear structure. Since the NLO testing of polar materials typically involves frequency multiplication from the near-infrared into the visible, the complexes should be transparent in the visible region. A SALEN [*N,N'*-ethylenebis(salicylaldiminato)] ligand was chosen to occupy the four equatorial positions (shown as an ellipse in Figure 1) because of its low optical absorption in the visible portion of the spectrum and its propensity for planar coordination geometries. The anionic group holding the bridging ligand at the apex of the square pyramid is a carboxylate. The carboxyl group will donate a minimal amount of electron density to the metal, keeping it as Lewis acidic as possible.

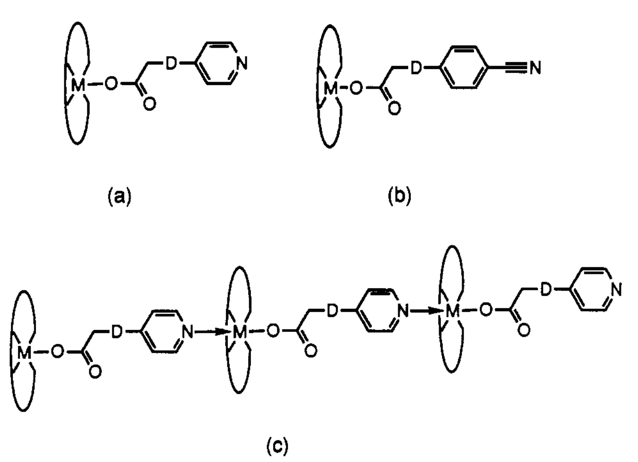

Figure 1. (a) Monomer units of **1** (D = NH) and **2** (D = S). (b) Monomer unit of **3**. (c) Coordination polymer formed from **1** or **2**. The ellipse represents a SALEN ligand.

Syntheses of the complexes were straightforward. (SALEN)MnBr and $^-O_2CCH_2DC_5H_4N$ (D = NH, S) were refluxed in methanol or water to give the desired products (**1** and **2**, respectively) (eq 2). A related complex was also prepared, in which the pyridyl has been replaced by a benzonitrile group. Displacement of bromide ion from (SALEN)MnBr by $^-O_2CCH_2NHC_6H_4C{\equiv}N$ in refluxing methanol gave **3** (eq 3).

$$(SALEN)MnBr + {}^-O_2CCH_2DC_5H_4N \rightarrow$$
$$(SALEN)Mn{-}O_2CCH_2DC_5H_4N + Br^- \qquad (2)$$
$$\mathbf{1}: D = NH$$
$$\mathbf{2}: D = S$$

$$(SALEN)MnBr + {}^-O_2CCH_2NHC_6H_4C{\equiv}N \rightarrow$$
$$(SALEN)Mn{-}O_2CCH_2NHC_6H_4C{\equiv}N + Br^- \qquad (3)$$
$$\mathbf{3}$$

Primary Structures of Polymers 1 and 2. The manganese(III) SALEN complexes **1** and **2** exist as infinite coordination polymers in the solid state. Thermal ellipsoid diagrams of the monomeric units for these polymers are shown in Figure 2, and selected bond distances and angles are given in Tables I and II. Comparison of the two thermal ellipsoid drawings shows that the two structures are nearly identical. The manganese atoms in both of these compounds possess octahedral coordination geometries with a SALEN ligand occupying four equatorial sites on the metal. One of the axial sites is occupied by a carboxylate oxygen atom and the other by a pyridyl nitrogen atom from an adjacent monomer. This bridging of adjacent monomers by the 4-pyridylglycinate and (4-pyridylthio)acetate ligands in **1** and **2**, respectively, results

---

(13) (a) Stults, B. R.; Marianelli, R. S.; Day, V. W. *Inorg. Chem.* **1975**, *14*, 722. (b) Cesari, M.; Neri, C.; Perotti, E.; Zazzetta, A. *J. Chem. Soc., Chem. Commun.* **1970**, 276. (c) Mathew, M.; Carty, A. J.; Palenik, G. J. *J. Am. Chem. Soc.* **1970**, *92*, 3197. (d) Hanack, M.; Deger, S.; Keppler, U.; Lange, A.; Leverenz, A.; Rein, M. *Synth. Met.* **1987**, *19*, 739.

(14) Wells, A. F. *Structural Inorganic Chemistry*, 4th ed.; Clarendon Press: Oxford, U.K., 1975.

(15) Bhattacharjee, S. K.; Ammon, H. L. *Acta Crystallogr., Sect. B* **1981**, *37*, 2082.

(16) Pollagi, T. P.; Stoner, T. C.; Dallinger, R. F.; Gilbert, T. M.; Hopkins, M. D. *J. Am. Chem. Soc.* **1991**, *113*, 703.

(17) Chisholm, M. H.; Hoffman, D. M.; Huffman, J. C. *Inorg. Chem.* **1983**, *22*, 2903.

(18) (a) Oudar, J. L. *J. Chem. Phys.* **1977**, *67*, 446. (b) Dulcic, A.; Flytzanis, C.; Tang, C. L.; Pepin, D.; Fetizon, M.; Hoppilliard, Y. *J. Chem. Phys.* **1981**, *74*, 1559. (c) Cheng, L. T.; Tam, W.; Marder, S. R.; Steigman, A. E.; Rikken, G.; Spangler, C. W. *J. Phys. Chem.* **1991**, *95*, 10643.

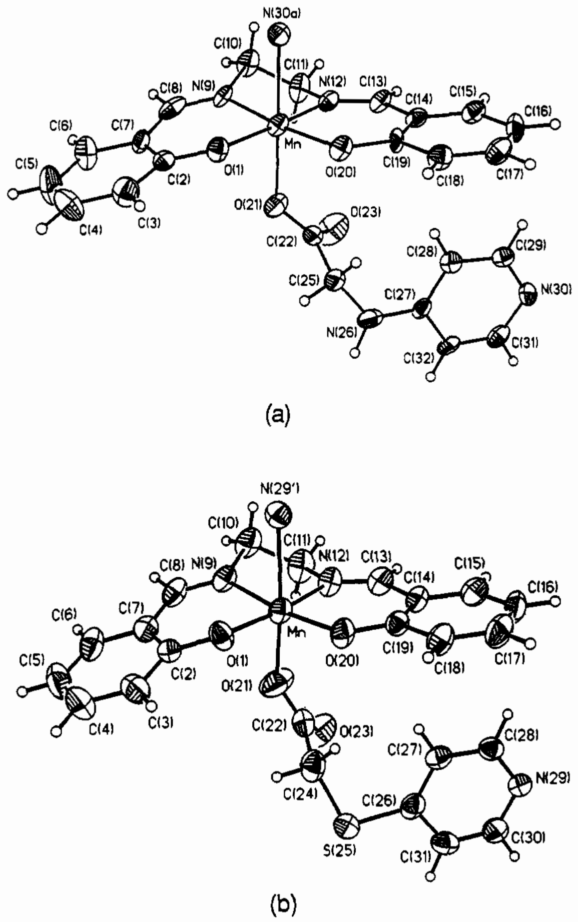

(a)

(b)

Figure 2. Thermal ellipsoid plots of the monomeric units of **1** (a) and **2** (b).

in the formation of infinite polymeric chains within crystals of these materials. Crystals of **1** and **2** also contain waters of hydration, and methanol is also observed in the lattice of **1**.

The structural features of the Mn(SALEN) units in these compounds are in good agreement with each other and with values reported for related Mn(III) Schiff base complexes.[19] The Mn–N(SALEN) distances are 1.993(7) and 1.997(7) Å for **1** and 1.980(5) and 1.990(4) Å for **2**, while the Mn–O(SALEN) distances are 1.897(5) and 1.898(6) Å for **1** and 1.891(4) and 1.894(3) Å for **2**. For comparison, the Mn–N and Mn–O distances in Mn(SALEN)(*p*-nitrobenzenethiolato) are 1.970(2) and 1.988(2) Å and 1.875(1) and 1.883(1) Å, respectively.[20] The conformation of the Mn(SALEN) units is also normal, with the stepped conformation being observed in both **1** and **2**.[21] One end of the SALEN is folded away from the axial pyridyl ligand, making a dihedral angle of 162.7° with the MnN_2O_2 equatorial plane in **1**. The corresponding dihedral angle for **2** is 159.4°. The other end is folded toward the pyridyl with dihedral angles of 174.3° for **1** and 172.7° for **2**. The dihedral angles between the two ends of the SALENs are 13.0 and 15.6° for **1** and **2**, respectively.

Considerable structural variations are however observed in the axial bonds. The Mn–N(pyridyl) bonds in **1** and **2** are statistically different, and this is also true of the Mn–O(carboxylate) bonds. The Mn–N(pyridyl) distance is 2.309(7) Å in **1** and 2.437(4) Å in **2**, while the Mn–O(carboxylate) distances are 2.203(6) and 2.132(4) Å for **1** and **2**, respectively. For comparison, the Mn–N(pyridyl) distances in the related 1,2-bis(2-hydroxybenzamido)benzene complex are 2.42(2) and 2.48(2) Å.[22] The Mn–N(pyridyl) bond in **2** is in good agreement with the latter values and is quite normal. We attribute the shortening of the Mn–N(pyridyl) bond in **1** to predominantly electronic effects. The electron-donating ability of an amino substituent at the 4-position of a pyridyl ring is known to increase the basicity of the ring nitrogen.[23] Hence, the pyridyl nitrogen of the 4-pyridylglycinate ligand would be expected to form a stronger and shorter Mn–N(pyridyl) bond than would the (4-pyridylthio)acetate ligand, and this is in fact observed.[24] The Mn–O(carboxylate) bonds exhibit the opposite trend, consistent with the more electron-rich and polarizable nitrogen of the 4-pyridylglycinate having a slightly greater trans influence versus the ring nitrogen of the (4-pyridylthio)acetate ligand. We point out, however, that the carboxylate oxygen atoms also participate in hydrogen-bonding interactions and that these and other features of the secondary and tertiary structures of these polymers also make additional contributions to the observed difference in the Mn–O(carboxylate) bonds (vide infra).

The Mn atom in both of these compounds are bound to their carboxylate ligands in a syn conformation, with the Mn atoms significantly out of the planes defined by their carboxylate groups.

Table I. Selected Bond Lengths (Å) and Angles (deg) for **1**

Bond Lengths			
Mn–N(12)	1.997(7)	C(19)–O(20)	1.324(10)
Mn–O(20)	1.897(5)	O(21)–C(22)	1.269(11)
Mn–O(21)	2.203(6)	C(22)–O(23)	1.246(12)
Mn–N(30A)	2.309(7)	C(22)–C(25)	1.513(14)
C(10)–C(11)	1.495(12)	C(25)–N(26)	1.454(11)
C(11)–N(12)	1.483(11)	N(26)–C(27)	1.353(11)
N(12)–C(13)	1.282(10)	C(27)–C(28)	1.388(12)
C(13)–C(14)	1.429(12)	C(27)–C(32)	1.413(12)
C(14)–C(15)	1.406(11)	C(28)–C(29)	1.370(12)
C(14)–C(19)	1.422(13)	C(29)–N(30)	1.345(11)
C(15)–C(16)	1.381(13)	N(30)–C(31)	1.351(12)
C(16)–C(17)	1.398(14)	N(30)–Mn(A)	2.309(7)
C(17)–C(18)	1.366(12)	C(31)–C(32)	1.347(12)
C(18)–C(19)	1.409(12)		
Angles			
N(12)–Mn–O(20)	91.4(3)	C(14)–C(19)–C(18)	117.9(7)
N(12)–Mn–O(21)	87.8(3)	C(14)–C(19)–O(20)	124.1(7)
O(20)–Mn–O(21)	91.5(2)	C(18)–C(19)–O(20)	118.0(8)
N(12)–Mn–N(30A)	92.8(3)	Mn–O(20)–C(19)	129.1(6)
O(20)–Mn–N(30A)	89.9(2)	O(21)–C(22)–O(23)	124.2(9)
O(21)–Mn–N(30A)	178.5(2)	O(21)–C(22)–C(25)	116.3(8)
N(9)–C(10)–C(11)	107.0(8)	O(23)–C(22)–C(25)	119.4(8)
C(10)–C(11)–N(12)	107.4(7)	C(22)–C(25)–N(26)	115.3(8)
Mn–N(12)–C(11)	112.6(5)	C(25)–N(26)–C(27)	124.2(8)
Mn–N(12)–C(13)	126.4(6)	N(26)–C(27)–C(28)	124.7(8)
C(11)–N(12)–C(13)	120.7(8)	N(26)–C(27)–C(32)	119.6(8)
N(12)–C(13)–C(14)	125.9(8)	C(28)–C(27)–C(32)	115.7(6)
C(13)–C(14)–C(15)	118.0(8)	C(27)–C(28)–C(29)	120.2(8)
C(13)–C(14)–C(19)	122.6(7)	C(28)–C(29)–N(30)	124.4(8)
C(15)–C(14)–C(19)	119.4(8)	C(29)–N(30)–C(31)	114.6(7)
C(14)–C(15)–C(16)	121.8(9)	C(29)–N(30)–Mn(A)	119.1(6)
C(15)–C(16)–C(17)	117.9(8)	C(31)–N(30)–Mn(A)	125.8(6)
C(16)–C(17)–C(18)	122.1(8)	N(30)–C(31)–C(32)	125.2(8)
C(17)–C(18)–C(19)	120.9(9)	C(27)–C(32)–C(31)	119.8(8)

---

(19) (a) Li, X.; Percoraro, V. L. *Inorg. Chem.* **1989**, *28*, 3403. (b) Gohdes, J. W.; Armstrong, W. H. *Inorg. Chem.* **1988**, *27*, 1842. (c) Matsumoto, N.; Takemoto, N.; Ohyosi, A.; Okawa, H. *Bull. Chem. Soc. Jpn.* **1988**, *61*, 2984. (d) Davies, J. E.; Gatehouse, B. M.; Murray, K. S. *J. Chem. Soc., Dalton Trans.* **1973**, 2523. (e) Oki, A. R.; Hodgson, D. J. *Inorg. Chim. Acta* **1990**, *170*, 65.

(20) Gohdes, J. W.; Armstrong, W. H. *Inorg. Chem.* **1988**, *27*, 1842.

(21) Stepped, planar, and umbrella conformations have all been observed for metal SALEN complexes: Calligaris, M.; Nardin, G.; Randaccio, L. *Coord. Chem. Rev.* **1972**, *7*, 385.

(22) Bertoncello, K.; Fallon, G. D.; Murray, K. S. *Inorg. Chim. Acta* **1990**, *174*, 57.

(23) Katritzky, A. R. *Handbook of Heterocyclic Chemistry*; Pergamon Press: Oxford, U.K., 1985.

(24) Cotton, F. A.; Wang, W. *New J. Chem.* **1984**, *8*, 331.

(25) In those cases where the anti conformation is observed, it is often the result of chelation or other factors which modify the sterics of the binding: (a) Bang, E.; Monsted, O. *Acta Chem. Scand., Ser. A* **1982**, *36*, 353. (b) Matsumoto, N.; Imaizumi, M.; Ohyoshi, A. *Polyhedron* **1983**, *2*, 137. (c) Kato, M.; Ito, T. *Bull. Chem. Soc. Jpn.* **1986**, *59*, 285. (d) Bonadies, J. A.; Kirl, M. L.; Lak, M. S.; Kessissoglou, D. P.; Hatfield, W. E.; Pecoraro, V. L. *Inorg. Chem.* **1989**, *28*, 2037. (e) Bhula, R.; Collier, S.; Robinson, W. T.; Weatherburn, D. C. *Inorg. Chem.* **1990**, *29*, 4027.

Table II. Selected Bond Lengths (Å) and Angles (deg) for **2**

Bond Lengths

Mn–N(12)	1.980(5)	C(18)–C(19)	1.410(7)
Mn–O(20)	1.894(3)	C(19)–O(20)	1.315(6)
Mn–O(21)	2.132(4)	O(21)–C(22)	1.246(7)
Mn″–N(29)	2.437(4)	C(22)–O(23)	1.221(7)
C(10)–C(11)	1.508(8)	C(22)–C(24)	1.527(9)
C(11)–N(12)	1.485(7)	C(24)–S(25)	1.785(6)
N(12)–C(13)	1.279(6)	S(25)–C(26)	1.743(5)
C(13)–C(14)	1.446(7)	C(26)–C(27)	1.384(7)
C(14)–C(15)	1.410(7)	C(26)–C(31)	1.401(8)
C(14)–C(19)	1.415(8)	C(27)–C(28)	1.365(7)
C(15)–C(16)	1.374(8)	C(28)–N(29)	1.346(7)
C(16)–C(17)	1.383(9)	N(29)–C(30)	1.331(7)
C(17)–C(18)	1.363(8)	C(30)–C(31)	1.358(8)

Angles

N(29′)–Mn–N(12)	89.5(2)	C(14)–C(19)–O(20)	123.6(4)
N(29′)–Mn–O(20)	90.7(1)	C(18)–C(19)–O(20)	118.6(5)
N(12)–Mn–O(20)	91.6(2)	Mn–O(20)–C(19)	129.5(3)
N(29′)–Mn–O(21)	171.6(2)	Mn–O(21)–C(22)	140.5(3)
N(12)–Mn–O(21)	86.6(2)	O(21)–C(22)–O(23)	124.8(6)
O(20)–Mn–O(21)	96.8(2)	O(21)–C(22)–C(24)	115.7(5)
N(9)–C(10)–C(11)	107.0(5)	O(23)–C(22)–C(24)	119.5(5)
C(10)–C(11)–N(12)	107.0(4)	C(22)–C(24)–S(25)	117.2(4)
Mn–N(12)–C(11)	112.8(3)	C(24)–S(25)–C(26)	105.0(3)
Mn–N(12)–C(13)	127.0(4)	S(25)–C(26)–C(27)	127.9(4)
C(11)–N(12)–C(13)	120.0(5)	S(25)–C(26)–C(31)	116.6(4)
N(12)–C(13)–C(14)	124.9(5)	C(27)–C(26)–C(31)	115.4(5)
C(13)–C(14)–C(15)	117.5(5)	C(26)–C(27)–C(28)	120.3(5)
C(13)–C(14)–C(19)	123.0(4)	C(27)–C(28)–N(29)	124.3(5)
C(15)–C(14)–C(19)	119.5(5)	Mn″–N(29)–C(28)	121.6(3)
C(14)–C(15)–C(16)	120.7(6)	Mn″–N(29)–C(30)	123.5(4)
C(15)–C(16)–C(17)	119.7(5)	C(28)–N(29)–C(30)	114.9(4)
C(16)–C(17)–C(18)	121.0(5)	N(29)–C(30)–C(31)	125.0(5)
C(17)–C(18)–C(19)	121.3(6)	C(26)–C(31)–C(30)	120.0(5)
C(14)–C(19)–C(18)	117.8(4)		

The Mn out-of-plane distances are 1.68 Å for **1** and 1.21 Å for **2**. This conformation is the geometry of choice for these compounds and for complexes based on related macrocyclic ligands.[25] Steric interactions between the substituent of the carboxylate and the macrocycle itself are minimized by adopting the syn conformation rather than the alternate anti form. A recent study has shown that increasing the steric bulk at the α-position of a carboxylate favors the syn conformation and out-of-plane bonding.[26] Both the syn conformation and the out-of-plane bonding between the Mn atoms and their carboxylate ligands in **1** and **2** can be explained by steric interactions between their aminopyridyl and thiopyridyl substituents, respectively, and the Mn(SALEN) unit.

Last, we focus briefly on the structural aspects of the metal–pyridyl interactions in **1** and **2**. The rotation (θ) of the pyridyl ring off the vertical plane bisecting the halves of SALEN appears to be correlated to the degree of bending (τ) of SALEN away from the bound pyridyl (Figure 3). θ and τ for **1** are 17 and 81°, respectively, while the same angles are 21 and 68° for **2**. The implication is that the orientation of the pyridyl is more likely dictated by local intramolecular steric interactions, e.g., between one of the methylene groups and the pyridyl ring itself, than by crystal packing forces. A similar relationship between θ and τ values (small θ gives large τ) is observed in other (SALEN)M(py)X complexes, in which the SALEN ligand is in a stepped conformation.[27]

Secondary Structures of Polymers 1 and 2 and Hydrogen Bonding. As eluded to in the previous section, compounds **1** and **2** exist as coordination polymers in the solid state and their general structural features are essentially identical. As a brief overview before proceeding further, however, we mention that these polymers are linear ...ABABAB... chain molecules derived from two basic components [A = Mn(SALEN) and B = a pyridylcarboxylate ligand] and that each ligand B bridges two neighboring A components in a head-to-tail fashion, i.e. –Mn(OOC–py)Mn(OOC–py)Mn(OOC–py)–. Polymers **1** and **2** are therefore two-component systems containing two standard linkages [a Mn–N(pyridyl) bond and a Mn–O(carboxylate) bond].

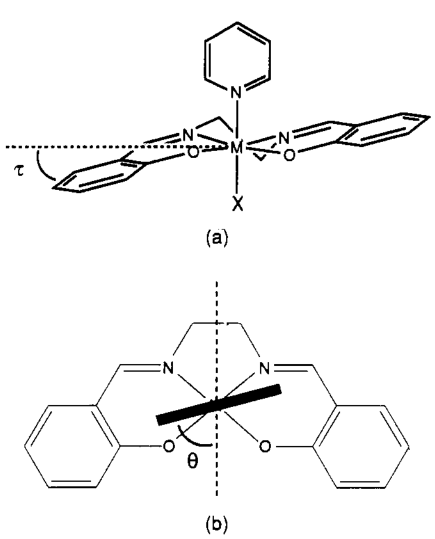

Figure 3. (a) Angle τ used to define the folding of the SALEN ligand away from the axial pyridyl group. (b) Angle θ used to describe the orientation of the pyridyl group. The heavy bar represents a pyridyl group viewed end-on.

Views of the polymer chains of **1** and **2** are given in Figure 4. The polymer chains are situated on 2-fold screw axes within the crystals. The Mn atoms are distributed about the polymer axis at distances of 1.65 Å in **1** and 1.60 Å in **2**. Both polymers possess a characteristic undulating backbone structure with adjacent Mn(SALEN) units oriented nearly perpendicular to one another within their respective chains. The MnN_2O_2 equatorial planes of adjacent Mn(SALEN) units are at dihedral angles of 83.1° in **1** and 82.4° in **2**. The angles between adjacent Mn–pyridyl dipoles within the polymer chains are 86.6 and 86.4° in **1** and **2**, respectively. The backbones exhibit the largest angular differences at the substituent atom on the 4-position of the pyridyl rings. The C(25)–N(26)–C(27) angle in **1** is 124.2(8)°, while the C(24)–S(25)–C(26) angle in **2** is considerably more acute at 105.0(3)°. This angular difference between the amino and thio groups is expected[28] but does not significantly alter the overall structural features of the polymer chains.

Changes in the interchain and hydrogen-bonding interactions in these polymers are however directly affected by the presence or absence of the 4-amino group on the pyridyl ring. A view of those interactions is given in Figure 4. Antiparallel chains of **1** are hydrogen-bonded through the 4-amino groups and solvent water molecules into a sheetlike structure vaguely reminiscent of the pleated sheets observed in polypeptides. Unlike those of polypeptides, alternate chains of **1** in these sheets are related by inversion symmetry rather than a 2-fold symmetry due to the synthetic nature of these materials. The distance between adjacent chain axes within the sheets is 11.0 Å, and the separation between the sheets is 6.09 Å. Adjacent chains in **2** are also arranged in an antiparallel fashion; however, interchain cross-linking is not observed. For comparison, the corresponding distances in **2** are 10.5 and 6.11 Å, respectively. Finally, the nonmetalated oxygen atoms of the carboxylate groups in these polymers participate in analogous hydrogen-bonding interactions, albeit with methanol in **1** and water molecules in **2**.

---

(26) Gorbitz, C. H.; Etter, M. C. *J. Am. Chem. Soc.* **1992**, *114*, 627.

(27) (SALEN)Ti(py)Cl: $\theta = 9°$, $\tau = 87°$ (Pasquali, M.; Marchetti, F.; Landi, A.; Floriani, C. *J. Chem. Soc., Chem. Commun.* **1978**, 545). (3-*t*-Bu-SALEN)Co(py)O_2: $\theta = 10°$, $\tau = 89°$ (Schafer, W.; Huie, B. T.; Kurilla, M. G.; Ealick, S. E. *Inorg. Chem.* **1980**, *19*, 340). (SALEN)Fe(py)N_3: $\theta = 23$, $\tau = 67°$ (Thompson, M. E.; Chiang, W.; Van Engen, D. Unpublished results.)

(28) (a) Chao, M.; Schempp, E. *Acta Crystallogr., Sect. B* **1977**, *33*, 1557. (b) Duclercq, P. J. P.; Germain, G.; Moreaux, C.; Van Meerssche, M. M. *Acta Crystallogr., Sect. B* **1977**, *33*, 3868.

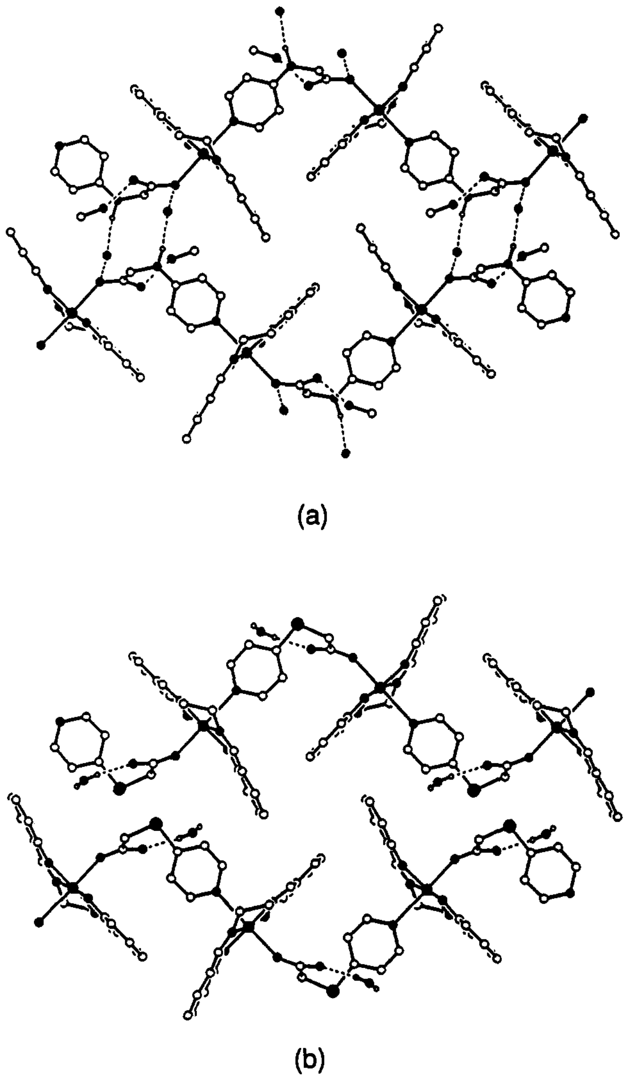

Figure 4. Perspective views of adjacent polymers of **1** (a) and **2** (b). Dashed lines indicate hydrogen-bonding interactions.

Primary Structure of 3. The major product isolated from the reaction of Mn(SALEN)Br and *N*-(4-cyanophenyl)glycine in methanol was recrystallized from water to give orange-brown crystals which analyze as $\mathrm{Mn(SALEN)L}\cdot{}^{1}/_{2}\mathrm{H_2O}$ where L denotes the *N*-(4-cyanophenyl)glycinate ligand. The X-ray structure of **3** revealed that it contains polymer chains of Mn(SALEN)L (**3A**) in intimate association with additional discrete molecules of Mn(SALEN)(H_2O)L (**3B**). The details of the X-ray analysis are presented below. The primary structural features of the polymer **3A** are examined first, followed by a discussion of the aquo complex **3B** and then, finally, the secondary structure and hydrogen bonding present in the solid state.

A view of the monomeric repeat unit in **3A** is shown in Figure 5a, and selected distances and angles are given in Table III. An additional view of a segment of the polymer itself is shown in Figure 6. Polymer **3A** is similar to **1** and **2** in that all three have structures based on octahedral Mn(III) with a SALEN ligand occupying four equatorial sites on the metal. One of the axial sites in **3A** is again filled by a carboxylate oxygen atom (in this case from the glycinate ligand L), while the remaining axial site serves as the point of attachment of a donor atom from a neighboring monomeric unit. In **1** and **2**, a pyridyl nitrogen atom is bound to the latter axial site to give the desired head-to-tail polymers. Our intent was to utilize the cyano nitrogen atom in L in an analogous fashion. As shown in Figure 6, however, that goal was not achieved. Instead, the remaining axial site is filled by a second carboxylate oxygen atom from a neighboring unit to give a polymer backbone based on a μ,η^2-bridged structure, i.e., –Mn[OC(R)O]Mn[OC(R)O]Mn[OC(R)O]–. The 4-cyanophenyl moiety does not participate in any bonding interactions with the Mn atoms. Figure 5b is a top view of the repeating unit of **3A** showing the relative positions of the benzonitrile ring with respect to the SALEN. The minimal distance of 3.45 Å between the benzonitrile and the salicylanilide ring (dihedral angle = 12°) suggests that there is a weak π–π interaction.

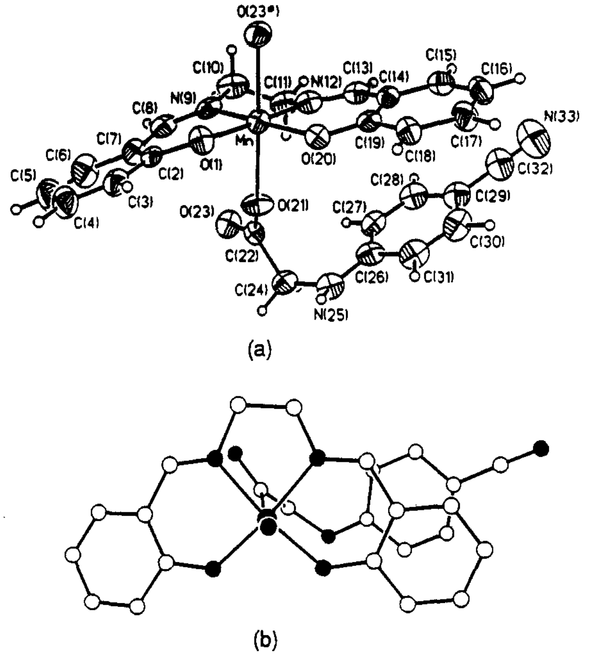

Figure 5. (a) Thermal ellipsoid plot of the monomeric unit of the Mn(SALEN)(*N*-(4-cyanophenyl)glycinate) polymer, **3A**. (b) Top view of the monomeric unit of **3A**.

The structural features of the Mn(SALEN) units in **3A** are similar to those reported earlier for the head-to-tail polymers. The Mn–N(SALEN) bonds are 2.004(6) and 1.978(6) Å, and the Mn–O(SALEN) distances are 1.879(5) and 1.904(5) Å. All of these are in the expected ranges and are in fair agreement with the values found for **1** and **2**. The Mn(SALEN) unit is again present in the stepped conformation and is folded to a slightly different degree due to the lack of the axial pyridyl group in the polymer. One end of the SALEN is folded toward the carboxylate O(21) atom and makes a dihedral angle of 20.0° with the MnN_2O_2 equatorial plane. The other end of the SALEN is folded toward the carboxylate O(23#) atom with a corresponding dihedral angle of 12.1°. The dihedral angle between the two ends of the SALEN is 9.3°.

The Mn–O(carboxylate) axial bonds are 2.273(5) and 2.268(5) Å and fall within the range 2.16–2.31 Å previously observed for related Mn(III) μ,η^2-carboxylate-bridged complexes.[29] The metal–carboxylate interactions are as expected on the basis of steric considerations. The Mn[μ,η^2-OC(R)O]Mn bridge in **3A** exhibits a syn-anti bonding pattern, in contrast to the anti-anti conformation exclusively observed in related Mn(III) complexes characterized by others.[29] It is important to note that all of the latter complexes contain acetate bridges such that steric conflicts in the anti positions would be expected to be fairly small. Substitution of a methyl hydrogen by the bulky *p*-cyanoaniline

---

(29) (a) Bonadies, J. A.; Kirl, M. L.; Lak, M. S.; Kessissoglou, D. P.; Hatfield, W. E.; Pecoraro, V. L. *Inorg. Chem.* **1989**, *28*, 2037. (b) Davies, J. E.; Gatehouse, B. M.; Murray, K. S. *J. Chem. Soc., Dalton Trans.* **1973**, 2523. (c) Akhtar, F.; Drew, M. G. B. *Acta Crystallogr., Sect. B* **1982**, *38*, 612. (Note: two of these references have appeared before: refs 27d, 20d.)

(30) The preference of the syn-anti conformation over the anti-anti geometry has been previously observed in Mn(II) amino acid complexes and a phenoxyacetate-bridged Mn(II) compound: (a) Ciunik, Z.; Glowiak, T. *Acta Crystallogr., Sect. B* **1981**, *37*, 693. (b) Clegg, W.; Lacy, O. M.; Straughan, B. P. *Acta Crystallogr., Sect. C* **1987**, *43*, 794. (c) Smith, G.; O'Reilly, E. J.; Kennard, C. H. L. *J. Chem. Soc., Dalton Trans.* **1980**, 2462.

Table III. Selected Bond Lengths (Å) and Angles (deg) for **3A** and **3B**

Bond Lengths

	3A	**3B**		**3A**	**3B**
Mn–N(12)	1.978(6)	1.977(6)	C(19)–O(20)	1.330(9)	1.324(9)
Mn–O(20)	1.904(5)	1.878(5)	O(21)–C(22)	1.265(8)	1.276(10)
Mn–O(21)	2.273(5)	2.179(5)	C(22)–O(23)	1.254(9)	1.229(10)
Mn–O(23#,34′)	2.268(5)	2.354(5)	C(22)–C(24)	1.526(11)	1.519(11)
C(10)–C(11)	1.505(11)	1.508(11)	C(24)–N(25)	1.435(10)	1.459(10)
C(11)–N(12)	1.476(9)	1.480(10)	N(25)–C(26)	1.367(11)	1.363(10)
N(12)–C(13)	1.280(10)	1.254(11)	C(26)–C(27)	1.396(11)	1.382(11)
C(13)–C(14)	1.446(10)	1.431(11)	C(26)–C(31)	1.418(12)	1.403(11)
C(14)–C(15)	1.393(10)	1.401(11)	C(27)–C(28)	1.368(12)	1.364(11)
C(14)–C(19)	1.417(10)	1.429(10)	C(28)–C(29)	1.415(12)	1.391(12)
C(15)–C(16)	1.377(11)	1.343(13)	C(29)–C(30)	1.368(13)	1.392(12)
C(16)–C(17)	1.385(12)	1.397(15)	C(29)–C(32)	1.435(13)	1.450(12)
C(17)–C(18)	1.368(11)	1.380(12)	C(30)–C(31)	1.362(13)	1.359(12)
C(18)–C(19)	1.413(10)	1.404(11)	C(32)–N(33)	1.140(13)	1.134(12)

Angles

	3A	**3B**		**3A**	**3B**
N(12)–Mn–O(20)	91.4(2)	92.4(2)	C(14)–C(19)–O(20)	123.8(6)	124.2(7)
N(12)–Mn–O(21)	90.2(2)	89.8(2)	C(18)–C(19)–O(20)	119.5(6)	118.4(6)
O(20)–Mn–O(21)	92.4(2)	102.3(2)	Mn–O(20)–C(19)	128.0(4)	127.9(4)
N(12)–Mn–O(23#,34′)	91.9(2)	86.2(2)	Mn–O(21)–C(22)	148.9(5)	132.3(5)
O(20)–Mn–O(23#,34′)	87.0(2)	89.7(2)	O(21)–C(22)–O(23)	125.6(7)	125.1(8)
O(21)–Mn–O(23#,34′)	177.9(2)	167.5(2)	O(21)–C(22)–C(24)	115.9(6)	116.2(7)
N(9)–C(10)–C(11)	107.9(6)	105.5(6)	O(23)–C(22)–C(24)	118.4(6)	118.7(7)
C(10)–C(11)–N(12)	108.2(6)	108.4(6)	C(22)–O(23)–Mn″	142.6(5)	
Mn–N(12)–C(11)	113.9(5)	112.8(5)	C(22)–C(24)–N(25)	117.0(6)	111.3(6)
Mn–N(12)–C(13)	126.1(5)	126.1(5)	C(24)–N(25)–C(26)	120.4(6)	125.4(6)
C(11)–N(12)–C(13)	119.9(6)	121.0(6)	N(25)–C(26)–C(27)	123.6(7)	122.8(7)
C(13)–C(14)–C(15)	117.3(7)	119.9(7)	C(27)–C(26)–C(31)	117.8(8)	117.9(7)
C(13)–C(14)–C(19)	122.2(7)	121.8(7)	C(26)–C(27)–C(28)	121.5(7)	121.3(7)
C(15)–C(14)–C(19)	120.1(7)	118.3(7)	C(27)–C(28)–C(29)	119.9(8)	120.6(7)
C(14)–C(15)–C(16)	121.8(7)	122.9(9)	C(28)–C(29)–C(30)	118.5(8)	118.6(8)
C(15)–C(16)–C(17)	118.2(7)	119.7(9)	C(28)–C(29)–C(32)	119.3(8)	120.3(8)
C(16)–C(17)–C(18)	121.5(7)	119.4(8)	C(30)–C(29)–C(32)	122.1(8)	121.1(8)
C(17)–C(18)–C(19)	121.6(7)	122.1(8)	C(29)–C(30)–C(31)	122.3(8)	120.5(8)
C(14)–C(19)–C(18)	116.7(7)	117.4(7)	C(26)–C(31)–C(30)	120.0(8)	121.1(8)
C(29)–C(32)–N(33)	178.0(10)	177.7(9)			

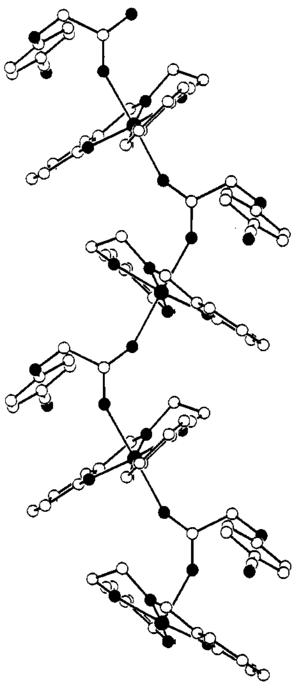

Figure 6. Perspective view of a polymer chain of **3A**.

group as in **3A**, however, should intensify such steric conflicts and eventually result in the anti-anti conformation falling into disfavor. Hence, in systems such as **3A**, the syn-anti conformation is in fact preferred and the bulky substituent is often seen rotated away from the sterically congested anti position and toward the less crowded syn side of the carboxylate bridge.[26,30] Both of the Mn atoms are displaced to the same side of the carboxylate plane with the syn-Mn and anti-Mn out-of-plane distances being 0.63 and 0.93 Å respectively.

The octahedral aquo complex **3B** is shown in Figure 7a, and selected distances and angles are given in Table III. As in **1**, **2**, and **3A** above, the four equatorial sites on the metal in **3B** are also involved in bonding to a SALEN ligand, and one of the axial sites is occupied by a carboxylate oxygen atom. The coordination sphere of the Mn atom is completed by the binding of a water molecule to the remaining axial position. Hence, the local environments of the Mn atoms in all of the complexes reported herein differ simply by having either a pyridyl (**1** and **2**), another carboxylate (**3A**), or a water molecule (**3B**) in the latter axial position. The Mn–N(SALEN) and Mn–O(SALEN) bonds are normal, and the Mn(SALEN) units in **3B** have a stepped conformation. One end of the SALEN is folded toward the carboxylate O(21′) atom and makes a dihedral angle of 21.6° with the MnN_2O_2 equatorial plane, and the other end is folded toward the water O(34′) atom with a dihedral angle of 10.8°. The dihedral angle between the two ends of the SALEN is 12.3°. The metal–carboxylate interaction may be described as having a syn conformation with the Mn atom 0.67 Å out of the carboxylate plane. The benzonitrile of **3B** is directed toward the ethylene bridge of the SALEN ligand, rather than a salicylanilide ring as seen in **3A** (Figure 7b). There are no close contacts between the benzonitrile and the SALEN ligand or those of adjacent molecules.

The $Mn–H_2O$ bond distances of 2.354(5) Å is among the longest observed in manganese complexes and is a particularly interesting feature of this compound. The occurrence of terminally bound water to a Mn(III) ion is considerably less common than the ubiquitous $Mn(II)–H_2O$ interaction. Typically, $Mn(III)–H_2O$ bonds are observed in the range 2.27–2.33 Å,[31] while Mn(II)–

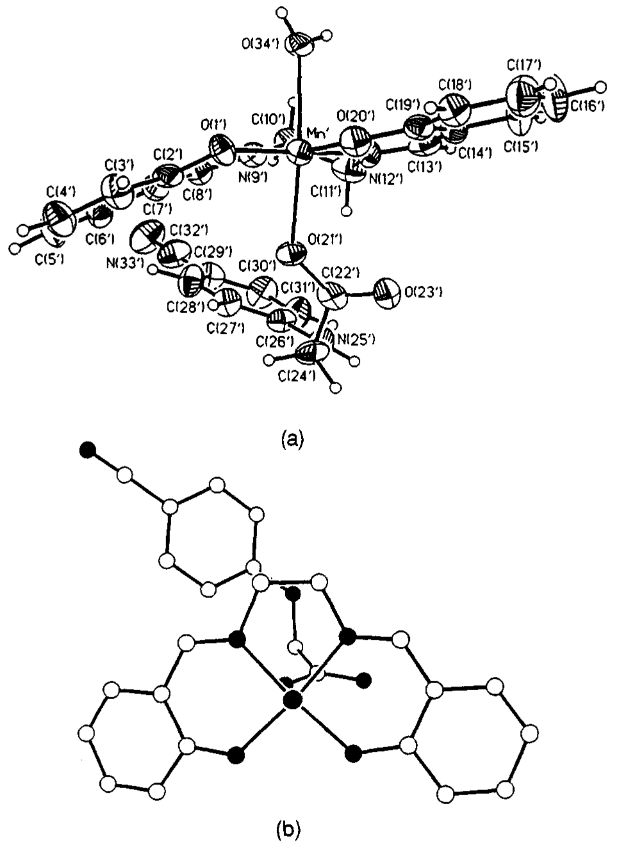

(a)

(b)

Figure 7. (a) Thermal ellipsoid plot of Mn(SALEN)(H_2O)(*N*-(4-cyanophenyl)glycinate), **3B**. (b) Top view of **3B**.

H_2O bonds occur at shorter distances averaging around 2.18(5) Å.[32] In octahedral complexes, a Jahn–Teller tetragonal elongation is often invoked to rationalize the lengthening observed in the Mn(III) high-spin d^4 systems.[19e,29,33] Presumably, a similar Jahn–Teller effect contributes to the long Mn(III)–H_2O bond observed in the present compound. We attribute the exceptionally weak binding of the water molecule and the added bond lengthening observed in **3B** to additional hydrogen-bonding forces in the crystal (vide infra).

Secondary Structure of 3. As discussed, the polymer **3A** consists of Mn(SALEN) moieties connected by a single carboxylate bridge in a syn-anti conformation (Figure 6). The polymer chain is situated on a 2-fold screw axis, very much like the polymers **1** and **2**. However, further structural comparison shows significant differences between these polymers. The Mn atoms are 0.52 Å off the polymer axis, which is considerably shorter than that found in **1** and **2**. The dihedral angle between adjacent Mn(SALEN) units is 71.9° compared to 86.6 and 86.4° found in **1** and **2**, respectively. Such differences are attributed to the shorter carboxylate bridge in **3A**. The short bridge enhances the steric interactions between the adjacent Mn(SALEN) units, forcing the dihedral angle to be more acute. Steric interactions are presumably also responsible for the marked difference in the orientation of the SALEN ligands of **3A** relative to the polymer backbone, compared to **1** and **2**. The long axis of the SALEN ligand lies perpendicular to the polymer backbone in **3A** but lies in the planes of the polymer backbones of **1** and **2** (see Figures 4 and 6).

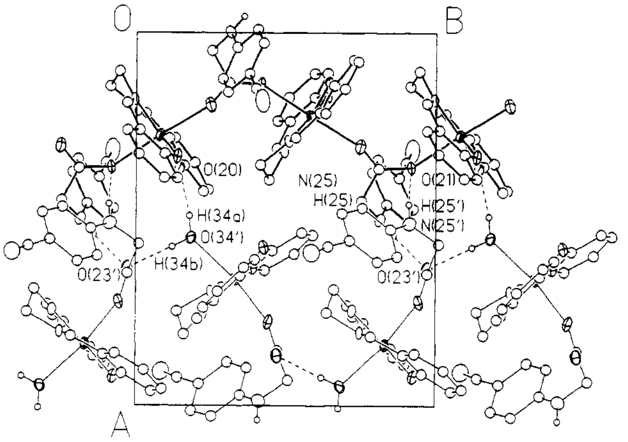

Figure 8. Perspective view of **3**, showing the relationship between the polymer Mn(SALEN)(*N*-(4-cyanophenyl)glycinate) (**3A**) and Mn(SALEN)(H_2O)(*N*-(4-cyanophenylglycinate) (**3B**) within the crystal. Dashed lines indicate the hydrogen-bonding interactions.

The relationship between **3A** and **3B** within the crystal is depicted in Figure 8. The polymer chain lies on the 2_1 axis parallel to *b* at ($^1/_4a$, $^3/_4c$), while the molecules of **3B** are distributed about the 2_1 axis parallel to *b* at ($^3/_4a$, $^3/_4c$). The benzonitrile groups of **3A** and **3B** are directed opposite each other. This arrangement results in two hydrogen bonds between **3A** and **3B**. A proton from an amine of **3B** is hydrogen-bonded to the carboxylate oxygen of the polymer [H(25′)···O(21)], and a proton from an amine of the polymer is hydrogen-bonded to a carbonyl oxygen of **3B** [H(25)···O(23′)]. This carbonyl oxygen is also hydrogen-bonded to the water molecule of an adjacent **3B** molecule [O(23′)···H(43b)]. Finally, the water molecule of **3B** is also hydrogen-bonded to one of the SALEN oxygens of the polymer [H(43a)···O(20)]. This hydrogen bonding network is repeated along both the *a* and *b* axes to generate the sheet shown in Figure 8. There is no hydrogen bonding between the sheets, and the distance between adjacent sheets is 13.6 Å.

Conclusion

The reaction between Mn(SALEN)Br and either *N*-4-pyridylglycine or (4-pyridylthio)acetic acid gave complexes which crystallize as coordination polymers. The monomeric unit consists of SALEN occupying the equatorial coordination sites of the metal, one axial site occupied by the carboxylate group, and the remaining axial site bonded to a pyridyl from an adjacent ligand. Comparisons between corresponding bond lengths and angles from the crystal structures show **1** and **2** to be essentially isostructural. The crystal structure revealed head-to-tail alignment of adjacent dipoles along a polymer backbone. Adjacent polymer chains in **1** are cross-linked by hydrogen bonds, whereas similar cross-linking was not observed for **2**. The polymer chains of both **1** and **2** lie in sheets in the crystals. Unfortunately, adjacent polymer chains are antiparallel; hence, no second-order nonlinear effects were observed.

Condensation between *N*-(4-cyanophenyl)glycine and Mn(SALEN)Br resulted in a compound which consists of polymer chains of Mn(SALEN)(*N*-(4-cyanophenyl)glycinate) cocrystallizing with molecules of Mn(SALEN)(H_2O)(*N*-(4-cyanophenyl)glycinate). Unlike the pyridyl groups in **1** and **2**, the benzonitrile of the polymer does not participate in any intermolecular bonding. Instead, adjacent Mn(SALEN) units are linked by the oxygen atoms of a single carboxylate. Each polymer strand is then flanked by the monomeric aquo complexes. As in **1**, sheets are formed by a hydrogen-bonding network and the crystal consists of the stacking of these sheets.

---

(31) (a) Lis, T.; Matuszewski, J.; Jezowska-Trzebiatowska, B. *Acta Crystallogr., Sect. B* **1977**, *33*, 1943. (b) Lis, T.; Matuszewski, J. *Pol. J. Chem.* **1980**, *54*, 163. (c) Menage, S.; Girerd, J. J.; Gleizes, A. *J. Chem. Soc., Chem. Commun.* **1988**, 431. (d) Mikuriya, M.; Nakadera, K.; Tokii, T. *Inorg. Chim. Acta* **1992**, *194*, 129.

(32) (a) Vreugdenhil, W.; Haasnoot, J. G.; De Graaff, R. A. G.; Nieuwenhuis, H. A.; Reefman, D.; Reedijk, J. *Acta Crystallogr., Sect. C* **1987**, *43*, 1527. (b) Ardiwinata, E. S.; Craig, D. C.; Phillips, D. J. *Inorg. Chim. Acta* **1989**, *166*, 233. (c) Goodson, P. A.; Oki, A. R.; Hodgson, D. J. *Inorg. Chim. Acta* **1990**, *177*, 59.

(33) (a) Lis, T. *Acta Crystallogr., Sect. B* **1978**, *34*, 1342. (b) Rettig, S. J.; Trotter, J. *Can. J. Chem.* **1973**, *51*, 1303.

Current work is in progress to incorporate chirality into the organic bridging ligand. One strategy is to use existing peptide synthetic methodologies to condense optically active amino acids with *N*-4-pyridylglycine or 4-(pyridylthio)acetic acid to give bridging ligands with chiral centers. The resulting coordination polymer will be guaranteed to crystallize in a noncentrosymmetric space group.

Experimental Section

Mn(SALEN)Br,[34] *N*-4-pyridylglycine hydrochloride,[35] and *N*-(4-cyanophenyl)glycine[36] were prepared according to literature procedures. (4-Pyridylthio)acetic acid and triethylamine were purchased from Aldrich and used without further purification. Methanol was of reagent grade.

IR spectra were obtained by a Nicolet 730 FT-IR spectrometer with resolution of 4 cm^{-1}. KBr was purchased from Aldrich and heated to 100 °C under vacuum for 12 h, after which it was stored in a 100 °C drying oven. The elemental analyses were performed on a Carlo Erba elemental analyzer (Model 1106).

1, Mn(SALEN)(*N*-4-pyridylglycinate). Mn(SALEN)Br (0.203 g, 0.5 mmol), *N*-4-pyridylglycine hydrochloride (0.094 g, 0.5 mmol), and triethylamine (0.150 g, 1.5 mmol) were refluxed in methanol (10 mL) for 5 h. The solid was collected by filtration, washed with methanol, and dried by suction until constant weight was observed (mp 232–234 °C, yield 61%). X-ray-quality crystals were obtained by slow evaporation of solvent from a saturated solution. IR (KBr): 3363 (s), 3237 (m), several small bands between 3200 and 2800, 1624 (vs), 1601 (vs), 1586 (vs), 1540 (s), 1533 (s), 1465 (w), 1444 (s), 1391 (s), 1365 (w), 1337 (m), 1298 (vs), 1266 (m), 1214 (s), 1198 (m), 1149 (m), 1127 (m), 1088 (w), 1034 (s), 990 (s), 901 (s), 795 (s), 759 (vs), 628 (s), 592 (m), 460 (s) cm^{-1}. Anal. Calcd for $C_{24}H_{27}N_4O_6Mn$: C, 55.18; H, 5.21; N, 10.72. Found: C, 55.50; H, 3.97; N, 11.04.

2, Mn(SALEN)((4-pyridylthio)acetate). (4-Pyridylthio)acetic acid (0.170 g, 10 mmol) was stirred into a mixture of distilled water (10 mL), methanol (5 mL), and triethylamine (1.500 g, 15 mmol) until all of the (4-pyridylthio)acetic acid had dissolved. Mn(SALEN)Br (0.406 g, 1 mmol) was then added, and the reaction mixture was heated to reflux for 6 h. The black solution was allowed to cool and filtered to give a black powder (mp 223–225 °C, yield 76%). Recrystallizing in water gave X-ray-quality crystals. IR (KBr): 3647 (vs), 2919 (m), several small bands between 3200 and 2700, 1623 (vs), 1598 (vs), 1585 (vs), 1541 (m), 1482 (w), 1464 (w), 1446 (s), 1414 (m), 1403 (w), 1388 (w), 1372 (s), 1332 (m), 1293 (m), 1248 (w), 1231 (w), 1216 (m), 1202 (m), 1148 (m), 1126 (m), 1110 (w), 1095 (w), 1047 (w), 1030 (w), 900 (m), 795 (m), 762 (s), 713 (w), 626 (m), 593 (w), 467 (s) cm^{-1}. Anal. Calcd for $C_{23}H_{22}N_3O_5SMn$: C, 54.44; H, 4.37; N, 8.28. Found: C, 53.67; H, 4.86; N, 8.08.

3, Cocrystal of Mn(SALEN)(*N*-(4-cyanophenyl)glycinate) (3A) and Mn(SALEN)(H₂O)(*N*-(4-cyanophenyl)glycinate) (3B). A mixture of Mn(SALEN)Br (0.800 g, 2 mmol), *N*-(4-cyanophenyl)glycine (0.350 g, 2 mmol), and triethylamine (0.600 g, 6 mmol) was refluxed in MeOH (25 mL) for 12 h. Cooling to room temperature gave a dark brown powder, which was collected by filtration, washed with methanol, and dried (mp 216–218 °C, yield 23%). Redissolving a sample in distilled water gave small black crystals which were used to seed another aqueous solution of 3, to obtain X-ray-quality crystals. IR (KBr): 3240 (s), 2208 (vs, –CN), 1642 (vs), 1627 (vs), 1603 (vs), 1549 (w), 1540 (m), 1528 (s), 1499 (w), 1466 (w), 1445 (s), 1391 (s), 1325 (w), 1302 (s), 1293 (s), 1270 (s), 1197 (w), 1171 (s), 1142 (s), 1126 (s), 1041 (w), 841 (w), 753 (vs), 627 (m), 465 (w), 459 (w) cm^{-1}. Anal. Calcd for $C_{50}H_{44}N_8O_9Mn_2$: C, 59.41; H, 4.39; N, 11.09. Found: C, 58.35; H, 3.80; N, 10.56.

Crystallography

Selected details pertaining to the X-ray analyses of **1**–**3** are summarized in Table IV. All of the diffraction experiments were performed on a Siemens R3m four-circle diffractometer employing graphite-monochromated Mo Kα radiation (λ = 0.710 73 Å). The samples were mounted on glass fibers with epoxy cement, and their lattice parameters were determined from the angular settings of well-centered high-angle reflections having 2θ values ranging out to 34°. All three samples were found to crystallize in the monoclinic space group $P2_1/c$ (No. 14). One quadrant of the data was collected at 213 K and out to 45° in 2θ for **1** and at 296 K and out to 50° in 2θ for **2**. A quadrant of data out to 50° in 2θ was also collected at 296 K for **3**, but in the space group $P2_1/n$ [an alternate setting of $P2_1/c$ (No. 14)]. Three standard reflections were monitored throughout each data collection, and no decomposition was detected. The data sets were corrected for Lorentz and polarization effects but not for absorption or extinction.

Table IV. Crystallographic Data for Compounds **1**–**3**

	1	**2**	**3**
formula	$C_{24}H_{27}MnN_4O_6$	$C_{23}H_{22}MnN_3O_5S$	$C_{25}H_{21}MnN_4O_4 \cdot C_{25}H_{23}MnN_4O_5$
cryst syst	monoclinic	monoclinic	monoclinic
space group	$P2_1/c$	$P2_1/c$	$P2_1/n$
a (Å)	10.782(2)	10.670(1)	14.295(4)
b (Å)	18.100(6)	17.754(3)	11.614(4)
c (Å)	12.886(4)	12.714(2)	27.220(7)
β (deg)	105.22(2)	108.78(1)	90.20(2)
V (Å^3)	2426.6(12)	2280.2(5)	4519.0(2)
Z	4	4	4
fw	521.4	507.4	1010.8
D(calcd) (Mg/m^3)	1.427	1.478	1.486
abs coeff (mm^{-1})	0.566	0.682	0.601
λ (Å)	0.710 73	0.710 73	0.710 73
T (K)	213	296	296
$R(F)^a$ (%)	7.48	5.73	7.18
$R_w(F)^b$ (%)	6.42	5.65	7.18

[a] $R(F) = \sum||F_o| - |F_c||/\sum|F_o|$. [b] $R_w(F) = [\sum w(|F_o| - |F_c|)^2/\sum w|F_o|^2]^{1/2}$.

The structure of **1** was solved by direct methods (XS: TREF), while those of **2** and **3** were solved by heavy-atom techniques (XS: PATT).[37] Full-matrix least-squares refinements were performed with anisotropic displacement coefficients for all of the non-hydrogen atoms and with the carbon-bound hydrogen atoms included at idealized positions. The oxygen-bound H atoms on the methanol and water molecules in **1** were not observed in any of the difference Fourier maps and were not included in any of the cycles of least-squares. The O-bound and N-bound hydrogens in **2** and **3** were taken from difference Fourier maps and included in subsequent refinements. In the former case of **2**, the coordinates for the H atoms of the water of hydration were free to vary without constraints. In the latter case of **3**, the N–H and O–H bonds present were constrained to 0.90 and 0.85 Å, respectively. The positional parameters for these hydrogens were otherwise also free to vary.

Acknowledgment. This work was supported the Air Force Office of Scientific Research (Grant AFOSR-90-0122) and the Advanced Technology Center for Photonics and Optoelectronic Materials (POEM, Princeton University).

Supplementary Material Available: Textual presentations of the structure determinations and complete tables of structure determination parameters, bond distances, bond angles, atomic coordinates, and thermal parameters for **1**, **2**, and **3** (39 pages). Ordering information is given on any current masthead page.

---

(34) Van Den Bergen, A.; Murray, K. S.; O'Connor, M. J.; West, B. O. *Aust. J. Chem.* **1969**, *22*, 39.

(35) Ohta, M.; Masaki, M. *Bull. Chem. Soc. Jpn.* **1960**, *33*, 1150.

(36) Peet, N. P.; Sunder, S. *J. Heterocycl. Chem.* **1977**, *14*, 561.

(37) (a) SHELXTL PLUS 4.11 for *R*3/*V* and *R*3*m*/*V* crystallographic systems: G. M. Sheldrick, University of Gottingen, Germany, and Siemens Analytical X-ray Instruments Inc., Madison, WI, 1990. (b) All computations were performed on a Microvax computer. (c) Neutral-atom scattering factors were used as stored in the SHELXTL PLUS structure determination package, and all non-hydrogen scattering factors were corrected for both the real and imaginary components of anomalous dispersion.